A Low-Complexity Linear-Phase Graphic Audio Equalizer Based on IFIR Filters

A Low-Complexity Linear-Phase Graphic Audio Equalizer based on IFIR Filters

V. Bruschi, S. Nobili, A. Terenzi, S. Cecchi, *Member, IEEE*

***Abstract*—Digital audio equalization is a very common procedure in the acoustic field that allows to improve the listening experience by adjusting the auditory frequency response. The design of graphic equalizers introduces several problems related to the necessity of implementing high performing filters with linear phase, usually characterized by high computational complexity. This paper proposes an innovative linear-phase graphic equalizer based on interpolated finite impulse response (IFIR) filters. IFIR filters seem to be suitable for a graphic equalizer thanks to their properties. In fact, they can reach very narrow transition bands, however with low computational complexity and linear phase, avoiding ripple between adjacent bands. The proposed IFIR equalizer has been compared with some state-of-the-art methods in terms of frequency response, distortion and computational cost. The experimental results have proved the effectiveness of the proposed equalizer, that has shown a considerable reduction on the computational complexity, meanwhile preserving the performances in terms of audio quality.**

***Index Terms*—audio equalization, audio systems, digital filters, digital signal processing, graphic equalizer, IFIR filters, linear phase**

I. INTRODUCTION

Equalization is a common process for sound reproduction that improves the listening experience by boosting or attenuating particular bands of the frequency spectrum. Graphic equalizers, so called because the sliders positions define a graph of the amplitude response, are commonly used [1]. This type of equalizer allows to adjust the gain in all the bands, maintaining the center frequencies and the quality factor, i.e., the ratio between the center frequency and the bandwidth, fixed. FIR filters are usually used to implement graphic equalizer as they ensure a linear phase. However, in all those cases where is required a high resolution of filters, the number of taps of FIR filters grows enormously. To improve the computational cost, a graphic equalizer using the fast convolution where the FIR filtering is implemented as a complex multiplication has been proposed in [2]. To reduce latency, Kulp has proposed [3] to divide the impulse response into segments and this method is quite efficient, as only one inverse FFT is needed if all the segments have the same length. In the literature, a large number of digital equalizers based on multirate filter-banks can be found. In [4], a tree structured filter-bank has been employed for a five band equalizer. The main problem of this structure lays in the delay that grows exponentially with the number of subbands. In [5], a digital filter-bank has been designed using frequency masking technique. This approach is greatly computationally efficient, but the delay becomes very large with stricter constraints. In [6], the Remez algorithm is applied in order to design filters of an 11-band linear-phase digital audio equalizer. The filters are calculated iteratively until reaching acceptable values of the deviation error. Therefore, this procedure requires a too high computational complexity. In [7], a linear-phase FIR equalizer based on multirate systems has been proposed and its real-time implementation has been presented in [8]. In particular, a near perfect reconstruction (NPR) cosine modulated filters bank [9] has been applied to audio fixed equalization. This approach has shown good performances, but a high computational cost. The system of [7] has been optimized in [10], [11] introducing IIR filters in order to reduce the computational complexity. Another graphic equalizer based on IIR filters is proposed in [12], which implements the cascade of second-order peak filters. However, these techniques do not guarantee a linear phase due to the IIR filters characteristics.

Focusing on the interpolated FIR (IFIR) filters, these filters achieve phase linearity and other strict design specifications, as small ripple and narrow transition bands, at moderate computational cost [13]. For this reason, they seem to be perfect for the construction of a computationally efficient graphic audio equalizer that overcomes the typical drawbacks described above. In [14], a method for small room equalization is proposed and a single IFIR filter is applied to the low frequencies. Instead, in [15], IFIR approach is applied for the realization of a graphic equalizer, but the presented tree structure cannot be automatically deployed considering a different number of bands.

In this paper, an innovative graphic equalizer based on IFIR filters is proposed considering a filter-bank structure. The main advantages of the proposed equalizer, which exploits IFIR filters, are: very narrow transition bands avoiding ripple between adjacent bands, low computational complexity and linear phase. Furthermore, the proposed structure and its attributes allow to design the filters once at first and change just the gains during the listening experience, avoiding continuous design of the filters.

The paper is organized as follows. Sec. II describes the design of the IFIR filter-bank. Sec. III shows the obtained results compared with some state-of-the-art equalizers, including through analysis on the computational complexity. Finally, in Sec. IV the conclusions are reported.

II. IFIR FILTER-BANK DESIGN

The proposed equalizer based on filter-bank structure is designed using IFIR filters that are composed of a cascade of two FIR filters [9]. The first FIR is designed from the model filter $F(z)$ applying an upsampling by a factor L, while the second FIR $G(z)$ is called interpolator which is

V. Bruschi, S.Nobili, A. Terenzi, S.Cecchi are with Università Politecnica delle Marche, Via Brecce Bianche, 60124 Ancona (e-mail: v.bruschi@univpm.it).

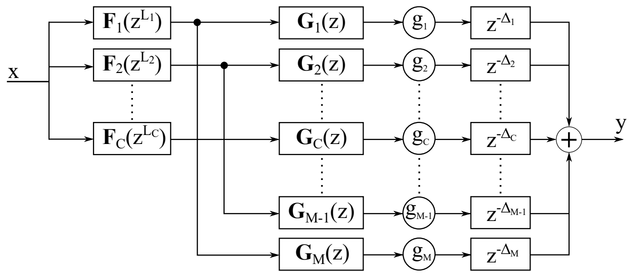

Fig. 1. Proposed equalizer scheme. The input signal x is filtered by $C = \lceil M/2 \rceil$ filters $F_i(z)$ interpolated by a factor L_i, with $i = 1, ..., C$. The output of $F_i(z)$ is the same for the i-th and the $(M - i + 1)$-th band. Then the filters $G_m(z)$, the gains g_m and the delays Δ_m are applied to each band, with $m = 1, ..., M$. The final output y is computed as the sum of the signal of each band.

designed to attenuate the unwanted copies of $F(z)$, due to the interpolation procedure. In the literature, several methods for the FIR filters design can be found. Some of the most classical techniques are the windowing approach [16] and the Parks-McClellan algorithm [17]. Other more recent methods allow to guarantee better performances and more control on the filter parameters, as discussed in [18], [19]. In this paper, the FIR filters $F(z)$ and $G(z)$ are designed using the Parks-McClellan algorithm [20], which allows to determine the order of the filter, knowing the specifications on the cut-off frequencies and ripples amplitude. IFIR filters ensure a lower computational cost and a narrower transition band than the simple FIR filters. In Fig. 1, the complete IFIR filter-bank scheme is reported, considering the model filter $F_i(z)$, the interpolation factor L_i, the interpolator $G_m(z)$, the assigned gain g_m and the applied delay Δ_m of the m-th band, with $m = 1, ..., C, ..., M$, $i = m$ for $m \leq C$ and $C = \lceil M/2 \rceil$, where M is the number of bands. The filters must be designed in pairs (the first with the last, the second with the second-to-last and so on), except for the central one. In fact, for each pair only a filter $F(z)$ is employed. The first and the last band consist of a low-pass and a high-pass filters, respectively, while the central bands consist of band-pass filters. In the following sections, the entire construction of the IFIR filter-bank is explained in detail.

A. First and last band of the equalizer

The first and the last band are obtained from the same filter $F_1(z)$. The normalized cut-off frequencies of the first low-pass filter are computed as follows:

$$\omega_{p,1} = \frac{\pi}{M} - \beta\Delta\omega, \tag{1}$$

$$\omega_{s,1} = \frac{\pi}{M} + (1-\beta)\Delta\omega, \tag{2}$$

where M is the total number of subbands, $\Delta\omega$ is the transition band and β is a parameter which can take values from 0 to 1 and establishes the overlap between nearby bands. Considering the Fig. 1, the filter $F_1(z)$ is a FIR filter with the following specifications:

$$F_1(z) : \begin{cases} \omega^F_{p,1} = L_1\omega_{p,1}, & \delta^F_p = \frac{\delta_p}{2} \\ \omega^F_{s,1} = L_1\omega_{s,1}, & \delta^F_s = \delta_s \end{cases}, \tag{3}$$

where δ_p and δ_s are the ripple in pass-band and stop-band respectively and the interpolation factor L_1 is the even value closest to L_{opt}, obtained as follows:

$$L_{opt} = \left\lfloor \frac{2\pi}{\omega_{s,1} + \omega_{p,1} + \sqrt{2\pi(\omega_{s,1} - \omega_{p,1})}} \right\rfloor. \tag{4}$$

The interpolated filter $F_1(z^{L_1})$ narrows the bandwidth of the low-pass filter and creates several images including a high-pass one, that defines the last band of the filter-bank, with the following cut-off frequencies:

$$\omega_{p,M} = \frac{\pi(M-1)}{M} + \beta\Delta\omega, \tag{5}$$

$$\omega_{s,M} = \frac{\pi(M-1)}{M} - (1-\beta)\Delta\omega. \tag{6}$$

Finally, the two filters $G_1(z)$ (low-pass) and $G_M(z)$ (high-pass) are computed as follows:

$$G_1(z) : \begin{cases} \omega^G_{p,1} = \omega_{p,1}, & \delta^G_p = \frac{\delta_p}{2} \\ \omega^G_{s,1} = \frac{2\pi}{L_1} - \omega_{s,1}, & \delta^G_s = \delta_s \end{cases}. \tag{7}$$

$$G_M(z) : \begin{cases} \omega^G_{p,M} = \omega_{p,M}, & \delta^G_p = \frac{\delta_p}{2} \\ \omega^G_{s,M} = \pi - \frac{2\pi}{L_1} + \omega_{s,1}, & \delta^G_s = \delta_s \end{cases}. \tag{8}$$

B. Intermediate bands of the equalizer

The intermediate bands are characterized by band-pass filters with the following cut-off frequencies:

$$\omega_{sj,m} = \frac{\pi(m-2+j)}{M} + (-1)^j(1-\beta)\Delta\omega, \tag{9}$$

$$\omega_{pj,m} = \frac{\pi(m-2+j)}{M} + (-1)^{j+1}\beta\Delta\omega, \tag{10}$$

where $m = 2, ..., M-1$ and $j = 1, 2$ indicating the first and the second transition band respectively. Also in this case the interpolation factor L_m for $m < C$, is the even value closest to L_{opt}, obtained by the Eq. (4) considering the frequencies $\omega_{p2,m}$ and $\omega_{s2,m}$. As mentioned before, the filters are designed in pairs (the second with the second-to-last and so on) and for each pair a band-pass filter $F_i(z)$ is defined as follows:

$$F_i(z) : \begin{cases} \omega^F_{s1,i} = L_i\omega_{s1,i}, & \delta^F_s = \delta_s \\ \omega^F_{p1,i} = L_i\omega_{p1,i}, & \delta^F_p = \frac{\delta_p}{2} \\ \omega^F_{p2,i} = L_i\omega_{p2,i}, & \delta^F_p = \frac{\delta_p}{2} \\ \omega^F_{s2,i} = L_i\omega_{s2,i}, & \delta^F_s = \delta_s \end{cases}, \tag{11}$$

where $i = 2, ..., C-1$. For each band a filter $G_m(z)$ is applied, as shown in Fig. 1. These filters are designed as low-pass filters for the first half of the filter-bank and as high-pass filters for the second one, as follows:

$$G_i(z) : \begin{cases} \omega^G_{p,i} = \omega_{p2,i}, & \delta^G_p = \frac{\delta_p}{2} \\ \omega^G_{s,i} = \frac{2\pi}{L_i} - \omega_{s2,i}, & \delta^G_s = \delta_s \end{cases}, \tag{12}$$

$$G_k(z) : \begin{cases} \omega^G_{p,k} = \pi - \omega_{p2,i}, & \delta^G_p = \frac{\delta_p}{2} \\ \omega^G_{s,k} = \pi - \frac{2\pi}{L_i} + \omega_{s2,i}, & \delta^G_s = \delta_s \end{cases}, \tag{13}$$

where $i = 2, ..., C-1$ and $k = M - i + 1$.

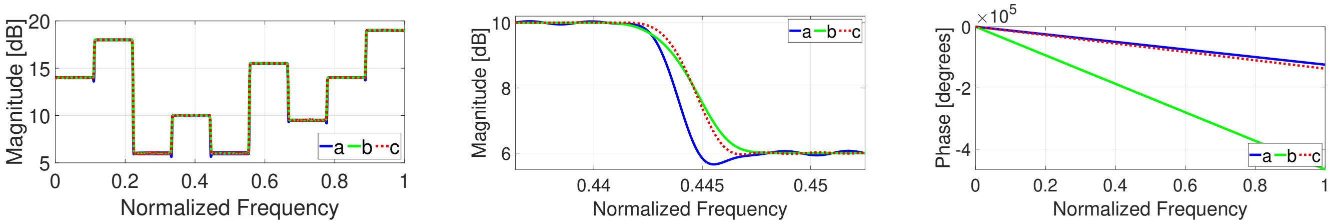

(i) (ii) (iii)

Fig. 2. (i) Magnitude response of the comparison between (a) the FFT equalizer, (b) the equalizer of [7] with $N_p = 1296$ and (c) the proposed equalizer considering $M = 9$ bands and $gain$ = [14 18 6 10 6 15.5 9.5 14 19] dB. (ii) Zoom on the transition of the fourth band of the previous comparison. (iii) Unwrapped phase response of the three considered equalizers.

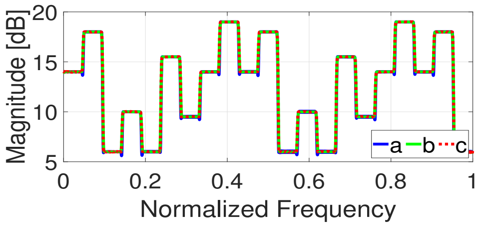

Fig. 3. Comparison between (a) the FFT equalizer, (b) the equalizer of [7] with $N_p = 1344$ and (c) the proposed equalizer considering $M = 21$ bands and $gain$ = [14 18 6 10 6 15.5 9.5 14 19 14 18 6 10 6 15.5 9.5 14 19 14 18 6] dB.

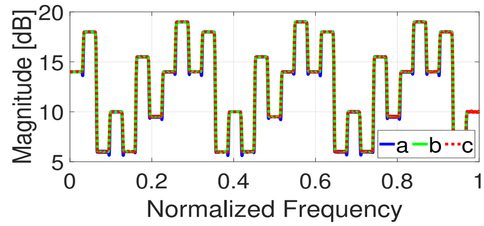

Fig. 4. Comparison between (a) the FFT equalizer, (b) the equalizer of [7] with $N_p = 1364$ and (c) the proposed equalizer considering $M = 31$ bands and $gain$ = [14 18 6 10 6 15.5 9.5 14 19 14 18 6 10 6 15.5 9.5 14 19 14 18 6 10 6 15.5 9.5 14 19 14 18 6 10] dB.

C. Central band of the equalizer

The central band is obtained from a low-pass filter $F_C(z)$ and an interpolation factor multiple of 4. The cut-off frequencies of the central filter are obtained following the Eq. (9)-(10) considering $m = C$. The interpolation factor L_C is the multiple of 4 closest to L_{opt} and less than L_{opt}, obtained following the Eq. (4) considering the frequencies $\omega_{p2,C}$ and $\omega_{s2,C}$. The low-pass filter $F_C(z)$ is designed following the equation:

$$F_C(z) : \begin{cases} \omega^F_{p,C} = L_C(\frac{\pi}{2} - \omega_{p1,C}), & \delta^F_p = \frac{\delta_p}{2} \\ \omega^F_{s,C} = L_C(\frac{\pi}{2} - \omega_{s1,C}), & \delta^F_s = \delta_s \end{cases}. \tag{14}$$

Finally, the band-pass filter $G_C(z)$ is designed as follows:

$$G_C(z) : \begin{cases} \omega^G_{s1,C} = \pi - \frac{2\pi}{L_C} - \omega_{s1,C}, & \delta^G_s = \delta_s \\ \omega^G_{p1,C} = \omega_{p1,C}, & \delta^G_p = \frac{\delta_p}{2} \\ \omega^G_{p2,C} = \omega_{p2,C}, & \delta^G_p = \frac{\delta_p}{2} \\ \omega^G_{s2,C} = \frac{2\pi}{L_C} + \omega_{s1,C}, & \delta^G_s = \delta_s \end{cases}. \tag{15}$$

D. Delay computation

The filters of the IFIR filter-bank have different lengths, so a delay is applied on each band. The delay of the m-th band introduced by the filtering process can be calculated as follows:

$$\tau_m = \frac{(\Lambda_m - 1)L_m + \Gamma_m - 1}{2}, \tag{16}$$

with $m = 1, ..., M$. Λ_m is the length of the m-th filter $F(z)$, Γ_m is the length of the m-th filter $G(z)$ and L_m is the m-th interpolation factor, considering that for $m > C$ the filters $F(z)$ and the respective interpolation factor L_m are the same as those defined for $m < C$, in accordance with the scheme of Fig. 1. The delay that must be applied for each band is computed as $\Delta_m = \tau_{\text{MAX}} - \tau_m$, where τ_{MAX} is the maximum delay among all bands.

III. Experimental Results

For the experimental tests, three different filter-banks have been designed varying the value of M, i.e., number of bands, with $M = 9$, $M = 21$ and $M = 31$. The proposed equalizer has been compared with the FFT-based equalizer [2], with the subband equalizer of [7], with the IIR equalizer of [12] and with the equalizer of [15] also based on IFIR. The parameters chosen for the proposed IFIR filter-bank are the following: transition band $\Delta\omega = 0.005\pi$, $\beta = 0.53$, pass-band ripple $\delta_p = 0.000575$, stop-band attenuation $\delta_s = 0.001$. The filter-bank of the FFT-based equalizer [2] has been designed imposing the same parameters of the proposed equalizer. The only difference is that each band is characterized by a single FIR filter designed with the Parks-McClellan algorithm [20]. Moreover, an FFT length of $N_{FFT} = 4096$ has been selected. For the subband equalizer of [7], the prototype filter length N_p has been chosen in order to obtain performances comparable to the proposed equalizer, so $N_p = 1296$ when $M = 9$, $N_p = 1344$ when $M = 21$ and $N_p = 1364$ when $M = 31$. The IIR equalizer of [12] has been computed using 10 peak/notch filters [21] for each band. In addition, also the 9-bands uniform equalizer of [15] has been considered, since it is based on IFIR filters. The approach of [15] is different from the proposed one and it is based on a tree structure built starting from a model filter and appropriate interpolation factors. For the comparison, two different lengths have been chosen for the model filter, $N_h = 13$ and $N_h = 161$, respectively.

For the proposed approach, the filters have been designed with double precision coefficients, avoiding quantization errors, since wordlengths greater than 16 bits do not degrade filters performance [22]. The comparison has been carried out considering a sampling frequency $f_s = 48$ kHz and evaluating the frequency magnitude response, the distortion index (DI) and the ripple, both reported in Table I, and the computational

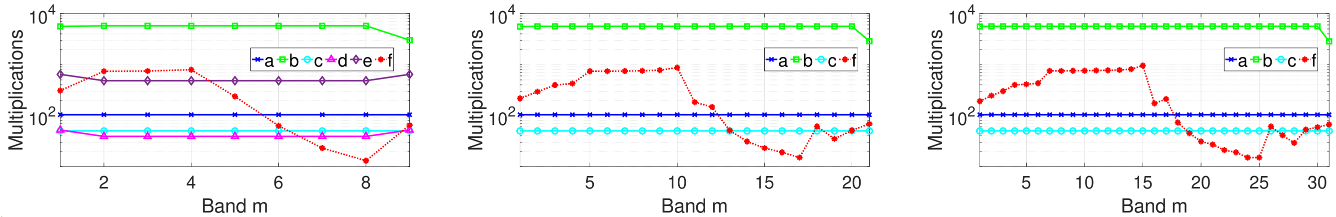

(i) (ii) (iii)

Fig. 5. Number of multiplication per input sample for each band in the case of (i) M=9, (ii) M=21 and (iii) M=31, comparing (a) the FFT equalizer, (b) the equalizer of [7], (c) the IIR equalizer of [12], (d) the IFIR equalizer of [15] with a model filter length of $N_h = 13$, (e) the IFIR equalizer of [15] with a model filter length of $N_h = 161$ and (f) the proposed IFIR equalizer.

TABLE I
DISTORTION INDEX AND RIPPLE EVALUATION

Equalizer	M=9		M=21		M=31	
	DI	Ripple	DI	Ripple	DI	Ripple
FFT-based [2]	0.9161	0.0881	0.9172	0.0878	0.9167	0.0886
Subband of [7]	0.9960	0.0043	0.9962	0.0042	0.9966	0.0043
IIR of [12]	0.9743	0.0419	0.9996	0.0159	0.9971	0.0134
IFIR of [15] N_h=13	1.0000	4.44e-16	-	-	-	-
IFIR of [15] N_h=161	1.0000	4.99e-16	-	-	-	-
Proposed	0.9988	0.0061	0.9993	0.0069	0.9998	0.0087

TABLE II
DELAY AND SLOPE EVALUATION

Band m	Proposed Equalizer		Equalizer of [15] N_h=13		Equalizer of [15] N_h=161	
	Delay [samples]	Slope [%]	Delay [samples]	Slope [%]	Delay [samples]	Slope [%]
1	761	18.19	90	1.22	1200	16.43
2	731	-48.94	66	-3.40	880	-44.91
3	735	18.61	78	1.35	1040	16.44
4	760	-18.69	78	-1.18	1040	-16.70
5	758	40.05	84	2.82	1120	35.67
6	760	-27.58	78	-1.85	1040	-24.66
7	735	19.53	78	1.40	1040	18.31
8	731	22.66	66	1.59	880	20.26
9	761	-	90	-	1200	-

cost, shown in Fig. 5. The distortion index has been defined as follows:

$$DI = \frac{\max|T(e^{j\omega})| + \min|T(e^{j\omega})|}{2}, \tag{17}$$

where $T(z)$ is the frequency response of the equalizer between 100 Hz and 23900 Hz, normalized for the value of the gain that is the same (10 dB) for all the bands. The DI evaluates the amplitude distortion of the frequency response and it should take values close to 1. Instead, the ripple has been calculated under the same conditions, but considering the difference between the maximum and the minimum of $T(z)$. Finally, the computational cost of the proposed equalizer has been evaluated in terms of number of multiplications Σ_m for each band, computed as follows:

$$\Sigma_m = \begin{cases} \Lambda_m + \Gamma_m & \text{for } m \leq C \\ \Gamma_m & \text{for } m > C \end{cases}, \tag{18}$$

where Λ_m and Γ_m are the length of the m-th filters $F(z)$ and $G(z)$, respectively. As shown by the Eq. (18), the filter $F(z)$ is considered only in the first half of the filter-bank. Analyzing the obtained results, the FFT-based equalizer of [2] presents the worst performances in terms of magnitude response (see Fig.s 2-4), DI and ripple. However, the computational cost of [2] is comparable with the average cost of the proposed equalizer in terms of multiplications. The subband equalizer of [7] has a magnitude response similar to the proposed equalizer (see Fig.s 2-4) and both the DI and the ripple are slightly smaller than the proposed method, but the computational cost is extremely high. The IIR based equalizer of [12] has the lowest computational cost and exhibits a DI very close to 1, similar to the DI of the proposed equalizer, despite a large value of the ripple. However, this is the only equalizer that does not guarantee a linear phase response due to the IIR characteristics. The 9-bands IFIR equalizer of [15] has been considered in the case of $N_h = 13$ and $N_h = 161$, where N_h is the length of the model filter. Looking at Table I, it seems the best performing when the same gain is applied to all bands. However, the transition bands are not very narrow when different gains are applied. This is a very important aspect since a high transition slope allows an accurate control of each individual band [23]. Steeper transition bands can be obtained choosing a longer model filter, increasing the delay and the computational cost. Table II reports the values of the slope of each transition band when the same gains of Fig. 2(i) are applied and the delay τ_m, comparing the proposed equalizer with [15]. The slope is calculated as the percentage value of the derivative of the magnitude curve (in dB) in correspondence of the center of the transition band. When the model filter is short, the equalizer of [15] presents a very small delay for each band, but the transition slope is too low. On the other hand, a filter length of $N_h = 161$ allows to obtain slope values similar to the proposed equalizer, but the delay dramatically increases. Moreover, also the computational cost raises with the filter length, as shown in Fig. 5(i).

To sum up, the proposed equalizer appears to be the best one reaching excellent values of DI and ripple and narrow transition bands, guaranteeing a low computational cost and a limited delay, maintaining a linear phase response, also increasing the bands number. More objective results can be found in [24]. Informal listening tests have also been carried out to evaluate perceptive effect of equalization. All involved subjects have reported positive comments on the perceived sound confirming the validity of the proposed approach.

IV. CONCLUSIONS

In this paper, an M-band uniform equalizer based on IFIR filters has been presented. The proposed method has been compared with other state-of-the-art equalizers. The experimental results have proved the effectiveness of the proposed IFIR equalizer that has reached great performances comparable to the state-of-the-art methods, showing extremely narrow transition bands and requiring a low computational cost. Future works may include a real-time implementation of the proposed equalizer for real-world experiments.

References

[1] V. Välimäki and J. Reiss, "All about audio equalization: Solutions and frontiers," *Applied Sciences*, vol. 6, p. 129, 2016.

[2] H. Schopp and H. Hetzel, "A Linear Phase 512 Band Graphic Equalizer using the Fast Fourier Transform," in *Proc. 96th Audio Engineering Society Convention*, Amsterdam, The Netherlands, Feb. 1994.

[3] B. D. Kulp, "Digital Equalization Using Fourier Transform Techniques," in *Proc. 85th Audio Engineering Society Convention*, Los Angeles, CA, USA, Oct. 1988.

[4] J. M. N. Vieira, "Digital five-band equalizer with linear phase," in *Audio Engineering Society Convention 100*, May 1996. [Online]. Available: http://www.aes.org/e-lib/browse.cfm?elib=7556

[5] Y. Lim, "A Digital Filter Bank for Digital Audio Systems," *IEEE Trans. Circuits Syst.*, vol. 33, no. 8, pp. 848–849, Aug. 1986.

[6] J. Henriquez, T. Riemer, and R. Trahan Jr., "A Phase Linear Audio Equalizer: Design and Implementation," *J. Audio Eng. Soc.*, vol. 38, no. 9, pp. 653–666, Sept. 1990.

[7] S. Cecchi, L. Palestini, E. Moretti, and F. Piazza, "A new approach to digital audio equalization," in *2007 IEEE Workshop on Applications of Signal Processing to Audio and Acoustics*, 2007, pp. 62–65.

[8] S. Cecchi, P. Peretti, L. Palestini, F. Piazza, F. Bettarelli, and A. Lattanzi, "Real time implementation of an innovative digital audio equalizer," in *Audio Engineering Society Convention 123*, Oct 2007. [Online]. Available: http://www.aes.org/e-lib/browse.cfm?elib=14366

[9] P. P. Vaidyanathan, *Multirate Systems and Filterbanks*. Prentice-Hall, Inc., 1993, ch. 4, pp. 134–143.

[10] M. Virgulti, S. Cecchi, and F. Piazza, "Iir filter approximation of an innovative digital audio equalizer," in *2013 8th International Symposium on Image and Signal Processing and Analysis (ISPA)*, 2013, pp. 410–415.

[11] M. Virgulti, S. Cecchi, A. Primavera, L. Romoli, E. Ciavattini, F. Bettarelli, and F. Piazza, "Optimized implementation of an innovative digital audio equalizer," in *Audio Engineering Society Convention 133*, Oct 2012. [Online]. Available: http://www.aes.org/e-lib/browse.cfm?elib=16535

[12] V. Välimäki and J. Liski, "Accurate cascade graphic equalizer," *IEEE Signal Processing Letters*, vol. 24, no. 2, pp. 176–180, 2017.

[13] Y. Neuvo, Dong Cheng-Yu, and S. Mitra, "Interpolated finite impulse response filters," *IEEE Transactions on Acoustics, Speech, and Signal Processing*, vol. 32, no. 3, pp. 563–570, 1984.

[14] F. Fontana, L. Gibin, D. Rocchesso, and O. Ballan, "Common pole equalization of small rooms using a two-step real-time digital equalizer," in *Proceedings of the 1999 IEEE Workshop on Applications of Signal Processing to Audio and Acoustics. WASPAA'99 (Cat. No.99TH8452)*, 1999, pp. 195–198.

[15] R. Hergum, "A low complexity, linear phase graphic equalizer," in *Proceedings of the 85th Audio Engineering Society Convention*, 1988.

[16] A. V. Oppenheim, R. W. Schafer, and J. R. Buck, *Discrete-Time Signal Processing*. Prentice Hall International Inc., 1999.

[17] T. Parks and J. McClellan, "Chebyshev approximation for nonrecursive digital filters with linear phase," *IEEE Transactions on Circuit Theory*, vol. 19, no. 2, pp. 189–194, 1972.

[18] L. San José Revuelta and J. Arribas, "A new approach for the design of digital frequency selective fir filters using an fpa-based algorithm," *Expert Systems with Applications*, vol. 106, 03 2018.

[19] J. Chen and Z. Cai, "A new class of explicit interpolatory splines and related measurement estimation," *IEEE Transactions on Signal Processing*, vol. 68, pp. 2799–2813, 2020.

[20] L. R. Rabiner, J. H. McClellan, and T. W. Parks, "Fir digital filter design techniques using weighted chebyshev approximation," *Proceedings of the IEEE*, vol. 63, no. 4, pp. 595–610, 1975.

[21] S. J. Orfanidis, *Introduction to Signal Processing*. Rutgers University, 2010, pp. 573-581.

[22] Xiaojuan Hu, L. S. DeBrunner, and V. DeBrunner, "An efficient design for fir filters with variable precision," in *2002 IEEE International Symposium on Circuits and Systems. Proceedings (Cat. No.02CH37353)*, vol. 4, 2002, pp. IV–IV.

[23] J. Rämö, V. Välimäki, and B. Bank, "High-precision parallel graphic equalizer," *IEEE/ACM Transactions on Audio, Speech, and Language Processing*, vol. 22, no. 12, pp. 1894–1904, 2014.

[24] "A3Lab - web site, other experimental results for IFIR innovative equalizer." http://www.a3lab.dii.univpm.it/research?layout=edit&id=90.